Conformational insights and vibrational study of a promising anticancer agent: the role of the ligand in Pd(II)–amine complexes

Sónia M. Fiuza, Ana M. Amado, Stewart F. Parker, Maria Paula M. Marques and Luís A. E. Batista de Carvalho

Published version information

Citation: Fiuza, SM et al. "Conformational insights and vibrational study of a promising anticancer agent: the role of the ligand in Pd(II)-amine complexes." New Journal of Chemistry, vol. 39, no. 8 (2015): 6274-6283.

doi: 10.1039/C5NJ01088H

A Conformational and Vibrational Study of a Promising Anticancer Agent: The Role of the Ligand in Pd(II)-Amine Complexes

Sónia M. Fiuza[*a], Ana M. Amado[a], Stewart F. Parker[b], M. Paula M. Marques[a,c] and Luís A. E. Batista de Carvalho[a]

[a]*Unidade de I&D "Química-Física Molecular", Departamento de Química, Universidade de Coimbra, Coimbra, Portugal.*

[b]*ISIS Facility, SFTC Rutherford Appleton Laboratory, Chilton, Didcot, OX 11 0QX, United Kingdom*

[c]*Departamento de Ciências da Vida, Universidade de Coimbra, Coimbra, Portugal*

[*]Correspondence author:
Tel./Fax: +351-239 826541
email: sonia.mfiuza@gmail.com

TOC

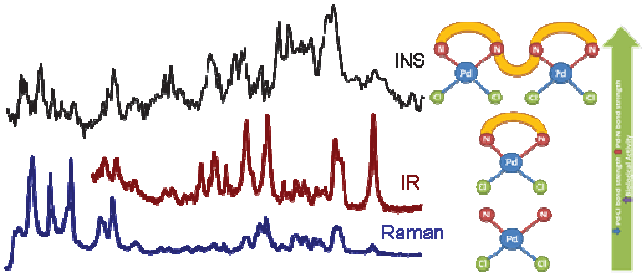

This study reports for the first time a complete vibrational analysis of a polynuclear amine-based compound with antiproliferative properties against cancer cells and the first steps on its Structure-Activity Relationship's (SARs).

Abstract

A conformational and vibrational analysis of an antiproliferative spermine-based polynuclear Pd(II) complex (Pd_2-Spm) is reported. Density Functional Theory coupled to all-electron basis sets was used to perform quantum mechanical calculations, aiming at determining the best suited strategy for accurately representing this molecule, and achieve an optimal accordance with the experimental data. The structural parameters and the vibrational frequencies predicted by the calculations are compared with the corresponding experimental data. The results support a relationship between the strength of the metal-ligand bonds and the antitumor activity of the compound.

Keywords

palladium(II); spermine; metal-ligand bond; anticancer; vibrational spectroscopy; quantum mechanical calculations

1. INTRODUCTION

Palladium(II) complexes are an emerging class of inorganic compounds bearing recognized anticancer properties,[1-5] challenging the initial belief that complexes containing this metal center would be inactive. This conviction started to materialize with the lack of biological activity of their parent compound *cis*-diamminedichloropalladium(II) (cDDPd),[6] as opposed to its Pt(II) homologue (cisplatin, *cis*-diamminedichloroplatinum(II), cDDP) that was justified by the higher lability of palladium(II) complexes relative to the platinum(II) ones. However, this problem has been circumvented by different synthetic strategies, most of them aiming at lowering this kinetic lability by coordination of the metal to polydentate or bulky ligands, yielding compounds with interesting therapeutic properties, largely determined by the nature of the ligands.[7-12] Kovala-Demertzi and co-workers[13] published an interesting study in which the substitution of a hydrogen for a methyl group in a bulky ligand has turned a biologically inactive compound into an active one. This shows that there is still a lot to be understood at the molecular level to unveil the physico-chemical phenomena that rule the behavior of these metal-based compounds in living systems – their structure-activity relationships (SAR's) being of paramount importance. Pd(II) complexes are particularly interesting compounds to perform SAR's studies, as the effect of the ligand on their biological activity is generally more pronounced than for their Pt(II) counterparts.

The present study focuses on a polynuclear Pd(II) chelate with a biogenic polyamine (spermine) – {μ-{N,N'-bis[(3-amino-κN)propyl]butane-1,4-diamine-κN:κN'}} tetrachloro-dipalladium (II), Pd_2-Spm (Figure 1.A).[14] This complex was shown to display interesting antiproliferative properties against cancer cells,[15,16] although it

presents a quite different chemical composition and structure from the array of active Pd(II) compounds reported in the literature to date. The understanding of the SAR´s ruling this type of compound's activity is fundamental for interpreting the biochemical mechanisms underlying their biological effect (*e.g.* cytotoxic), thus allowing a rational design of new Pd-based anticancer drugs. Vibrational spectroscopy has proven to be one of the most powerful techniques for performing conformational studies in biologically relevant molecules (including inorganic compounds). Inelastic neutron scattering (INS) spectroscopy is particularly well suited to study materials containing hydrogen atoms, since the scattering cross section for hydrogen (^{1}H) (about 80 barns) is much larger than for most other elements (at most *ca.* 5 barns). The neutron scattering cross-section of an element is a characteristic of each isotope and independent of the chemical environment. During the scattering event, a fraction of the incoming neutron energy can be used to cause vibrational excitation, and the vibrational modes with the largest hydrogen displacements will dominate the spectrum. Therefore, INS can be especially important in solids in which the molecular units are linked together by hydrogen close contacts, with the lowest-frequency vibrations expected to be most affected. Combining experimental vibrational spectroscopy results with quantum mechanical calculated data allows a deeper understanding of the correlation between the system's molecular properties (structure and conformation) and the corresponding spectra.

In this study, quantum mechanical calculations were carried out for Pd_2-Spm at the DFT level, since this approach has shown to deliver accurate results for this type of systems.[17-19] A theoretical model previously reported by the authors for a mononuclear Pd(II) compound bearing non-chelating ligands[17] was presently evaluated as to its suitability for the highly flexible polynuclear polydentate chelate Pd_2-Spm. The

accuracy of the calculated results was assessed by comparison with the experimental data available on this chelate – both reported X-ray structural information[14] and the vibrational results gathered in this work.

2. EXPERIMENTAL

2.1 Synthesis of Pd_2-Spm

Potassium tetrachloropalladate(II) (K_2PdCl_4, 98%) and spermine (≥97%) were acquired from Sigma (Sintra, Portugal) and used without further purification.

The synthesis of Pd_2-Spm was carried out following an optimized procedure based on the published synthetic route.[14] Briefly, 2 mmol of K_2PdCl_4 were dissolved in a minimal amount of water, and an aqueous solution containing 1 mmol of spermine was added drop wise under continuous stirring, for about 24 h. Solid $(PdCl_2)_2$(Spm) was formed, which was filtered and washed with pure acetone. Upon drying in an oven at 40ºC overnight yellow crystals were obtained.

Yield: 68%. Elemental analysis was carried out at the Atlantic Microlab, Inc., Georgia, USA. Calculated - C: 21.56%; H: 4.70%; N: 10.06%, Cl: 25.46% and Found: C: 21.22%; H: 4.68%; N: 9.60%, Cl: 25.88%.

2.2 Vibrational Spectroscopy

Room-temperature Fourier transform Raman (FT-Raman) spectra were acquired on an RFS-100 Bruker Fourier transform Raman spectrometer, with near-infrared excitation provided by the 1064 nm line of a Nd:YAG laser. A laser power of 150 mW at the sample position was used. Each spectrum was the average of three repeated measurements of 150 scans, at 2 cm^{-1} resolution.

The Fourier transform infrared (FTIR) spectra at room-temperature were recorded over the 400-4000 cm^{-1} region, on a Mattson 7000 FTIR spectrometer, using a globar source, a deuterated triglycine sulfate (DTGS) detector and potassium bromide pellets. Each spectrum was composed of 32 scans, with 2 cm^{-1} resolution and triangular apodization.

The INS spectrum of the complex was obtained at the ISIS Pulsed Neutron Source of the STFC Rutherford Appleton Laboratory (United Kingdom), using the TOSCA spectrometer, an indirect geometry time-of-flight, high resolution (*ca.* 1.25% of the energy transfer), broad range spectrometer.[20] A crystalline sample of the complex (2-3 g) was wrapped in a 4×4 cm aluminium foil sachet, which filled the beam, and placed in a thin walled aluminium can. To reduce the impact of the Debye-Waller factor on the observed spectral intensity, the sample was cooled to *ca.* 15 K. Data was recorded in the energy range -24 to 4000 cm^{-1} and converted to the conventional scattering law, $S(Q, \nu)$ *vs* energy transfer (in cm^{-1}) through standard programs.

2.3 Computational Details

All calculations were performed using the Gaussian 03W (G03W) package.[21] Both isolated molecule and two-molecule geometry were fully optimized by the Berny algorithm, using redundant internal coordinates. While the initial conformational study was carried out without symmetry constraints, once the best conformer was selected subsequent calculations were subject to symmetry constraints (C_i symmetry group). The optimization convergence criteria for the cut-offs of forces and step sizes were: 0.000450 Hartree/Bohr for maximum force, 0.000300 Hartree/Bohr for root-mean-

square force, 0.001800 Bohr for maximum displacement and 0.001200 Bohr for root-mean-square displacement. In all cases, vibrational frequency calculations were performed, at the same level of theory, to verify that the geometries corresponded to a real minimum in the potential energy surface (no negative eigenvalues) and to simulate the vibrational spectra.

Two approaches were used to describe the palladium atom: by relativistic pseudopotentials developed by Hay and Wadt,[22] in a double-zeta splitting scheme, as implemented in G03W (keyword *LANL2DZ*); or by an all-electron (AE) contracted Gaussian basis set developed by Friedlander.[23] Inclusion of a polarization function at the Pd atom, by augmenting the valence shell with an f-function (ζ_{Pd}=1.472), was also tested in combination with LANL2DZ.[24] For the non-metal atoms, several AE basis were tested: 6-31G*, 6-31G**, 6-31+G(2d) and 6-31+G(2df) (as defined in G03W), either alone or simultaneously in distinct combinations schemes for different atoms (mix 1 and mix 2), as described in Table 1. Natural Bond Orbital (NBO) analysis was also performed. The basis sets were tested at the DFT theory level, using the mPW1PW method which comprises a modified version of the exchange term of Perdew-Wang and the Perdew-Wang 91 correlation functional,[25,26] which has been shown to be advantageous over other DFT functionals for both linear amine ligands and their Pt(II)/Pd(II) complexes.[17,18,27] The B97D DFT, which includes semi-empirical corrections for dispersion, was also tested.[28] In order to account for the basis set superposition error (BSSE) in the two-molecule model calculation, geometries were optimized within the scheme of Boys-Bernardi[29] (as implemented in G03W, by use of the keyword counterpoise).

3. Results and Discussion

3.1 Conformational analysis

The reported X-ray structure for the Pd_2-Spm molecule[14] (Figure 1) comprises both Pd(dap)Cl_2 units (dap=1,3-diaminopropane, $H_2N(CH_2)_3NH_2$)) in a relative *trans* arrangement. The chelate ring assumes a chair conformation, while the central putrescine-like moiety has an all-*trans* geometry. Careful inspection of this crystalline lattice structure (Figure 1.C) suggests the formation of intermolecular H-bonds between the Pd(dap)Cl_2 fractions of adjacent molecules, namely Cl_1;$Cl_2\cdots H_1$,$H_2(N_1)$ and $Cl_2\cdots H_9(N_2)$, as well as a $Cl_1\cdots H_{10}(C_4)$ interaction. The more hydrophobic methylene groups, in turn, should not be involved in this type of close contacts.

A full conformational analysis was performed for the Pd_2-Spm isolated molecule (Figure S1 of the supplementary material), in the light of previous work on the cDDPd mononuclear complex.[17]. The minimum energy conformer obtained for Pd_2-Spm differs significantly from the reported X-ray structure, which suggests that, this type of single molecule conformational studies may not be adequate to accurately represent these large polynuclear systems, since the intermolecular interactions between neighboring molecules in the crystal lattice (Figure 1.C) impact on their structure to a much larger extent than for mononuclear complexes playing an non-negligible role on the maintenance of the overall chelate´s conformation.

Although plane-wave calculations have been carried out by the authors[30-33] to predict solid state arrangements, this type of approach is not easily accessible for this particular dinuclear chelate due to the large dimensions of the corresponding unit cell. In view of these limitations, and taking into account that the aim of this study is to predict the properties of Pd_2-Spm in the solid state, the lowest-energy conformer found for the isolated molecule (conformer 1, Figure S1) was not considered in further

analysis, but rather the optimized Pd_2-Spm isolated molecule that matches the X-ray data (conformer 5, Figures 1.A).

3.2 Structural analysis

The selected conformer (conformer 5, Figure 1.A) for Pd_2-Spm was reoptimized under symmetry constraints (C_i symmetry group), yielding the structural parameters comprised in Table 2. Also presented are the difference between the experimental and calculated values (Δ-values), and the corresponding overall errors (ΔΔ-values), calculated as previously described for cisplatin[18]. In general, the larger deviations from the experimental values are verified for the $Pd(dap)Cl_2$ moiety. It was hypothesized that these could be mainly due to: (i) poor description of the metal center and/or (ii) neglecting the intermolecular interactions present in the crystal lattice.

Considering hypothesis (i), the LANL2DZ ECP was augmented with an f-polarization function at the Pd center, and the all-electron basis set of Friedlander[23] was tested in the metal ion. While augmenting the Pd valence shell did not lead to a significant change (results not shown), the use of an AE basis at the Pd ion caused clear changes in the complex´s structural parameters. From analysis of Table 2, it is evident that the use of an AE basis set on Pd(II) greatly improves the prediction of the Pd-N bond length, which had been previously overestimated by all theoretical approaches. However, this leads to a worsening of the Pd-Cl bond length values (as well as of some bond angles involving chlorine), in the order: for the Pd-Cl bond, LANL2DZ/6-31G* > AE/mix1 > AE/6-31G*~AE/mix2 > AE/6-31G+(2d) > AE/6-31G**; for the Cl-Pd-Cl angle, LANL2DZ/6-31G* > AE/6-31G** > AE/mix2 > AE/mix1~AE/6-31G* > AE/6-31G+(2d); for the Cl-Pd-N angle, LANL2DZ/6-31G* > AE/6-31G** > AE/mix2 > AE/mix1~6-31G* > AE/6-31G+(2d). Interestingly, the addition of a polarization

function to the hydrogen atom (AE/6-31G* → AE/6-31G**) leads to a better overall agreement relative to the experimental values of the Cl-Pd-Cl and N-Pd-Cl angles, which can probably be due to a better description of the neighboring molecular groups bearing hydrogens. However, including higher polarization functions on the non-hydrogen atoms (AE/6-31+G(2d)) did not lead to an enhancement of the overall ΔΔ values. Coupling the AE basis set tested for Pd(II) with a combination of different AE basis sets for the remaining atoms (mix1 or mix2) yielded better ΔΔ values but did not solve the problem entirely. While mix1, which involves more extensive basis sets for the chlorine and nitrogen atoms (Table 1), led to a significant improvement of the Pd-Cl bond length, it did not produce more accurate values for the bond angles. In turn, while mix2, which extends the improvement of the basis set to the carbon, chlorine and nitrogen atoms (Table 1), yields better Δ values for the angles, it worsens some of the bond lengths.

Regarding hypothesis (ii), calculations for a two-molecule species (Figure S2, supplementary material) based on the X-ray structure reported for the complex, were performed to verify if accounting for intermolecular interactions could improve the results. Considering this model led to an improvement of the calculated Pd-N bond length, at the cost of a worsening of the values for the Pd-Cl bond (Table S1, supplementary material). However, although the bond angles involving the metal center were greatly improved, the overall error was not much lower than that obtained for the isolated molecule. The reason for this probably lies on the fact that only two Pd_2-Spm molecules are not enough to represent all the intermolecular interactions occurring in the solid lattice, where one Pd_2-Spm entity is surrounded by six neighboring molecules (Figure 1.C). Accounting for a six-molecule model using the present theoretical

approach is, however, not feasible. A calculation for the two-molecule structure was also performed with the new B97D DFT, which accounts for dispersion corrections allowing a better description of the intermolecular interactions, but without significant improvement in the results (not shown).

The theoretical estimate of the chelate´s structural parameters is of the utmost importance for the prediction of reliable SAR's for the complex. When comparing the experimental bond lengths for different compounds of the same type, it is interesting to verify that within Pd_2-Spm the Pd-N bonds (203.2 pm average value, Table 2) are shorter relative to the parent mononuclear compound cDDPd (206.0 pm)[34], while the Pd-Cl ones are longer (231.5 pm *vs.* 227.5 pm).[34] Natural Bond Orbital (NBO) calculations through the calculated Wiberg bond indexes - an indicator that reflects the strength of the bond - also predict this trend which is interestingly correlated with the biological activity of the complexes involved (Figure 2).

The mode of action of this type of metal-based compounds is recognized to be interaction and binding to DNA.[35,36] Although the exact mechanism for Pd(II) complexes is not as well established as for their Pt(II) analogues, they are expected to have a rather similar behavior due to their similar chemical characteristics. The anticancer properties of the well-known chemotherapeutic drug cisplatin relies on the binding of Pt(II) to the nitrogen (N^7) of the DNA bases.[35-37] This step must be preceded by an intracellular drug activation process through aquation, that involves the hydrolysis of the chlorine ligands. Accordingly, it is expected that the DNA binding ability of these amine-based Pd(II) complexes increases with weakening of the Pd-Cl bonds, as evidenced in Figure 2.

3.3 Vibrational analysis

Pd_2-Spm has 132 vibrational modes, 66 of A_u symmetry (infrared active) and 66 bearing A_g symmetry (Raman active). All the modes are INS active, since there are no selection rules for this non-optical vibrational spectroscopy technique (Figure 3).

The assignment of the vibrational spectra of Pd_2-Spm, as well as the calculated wavenumbers at the LANL2DZ/6-31G* theory level, has it has been shown previously that the small enhancement obtained with higher theory levels is not worth the associated computational cost,[17,18] are presented in Table 3. Some vibrational modes (as well as the corresponding nomenclature used throughout the text) are schematically represented in Figure 4. As the metal units are linked by the aliphatic amine spermine, some low frequency vibrations are similar to the reported LAM and TAM modes previously assigned for this polyamine.[39,40] However, they were given alternative designations in this work since Pd-coordinated Spm does not constitute a free "linear bead system".

The vibrational modes from the spermine ligand were reasonably predicted by the calculations, despite some deviations due to anharmonicity and/or intermolecular interactions. The major differences were verified for the modes involving the atoms directly bound to the metal atom, which cannot be justified in terms of anharmonicity since there is not a uniform pattern in the prediction of the wavenumbers. In order to determine whether this was a particular effect of this chelate, calculations were performed, at the same theory level (LANL2DZ/6-31G*), for a few other Pd(II) complexes with different amine ligands. The data thus gathered is collected in Table 4 as the scaling factor needed to match the calculated wavenumbers to the experimental ones. In every case, the theoretically predicted Pd-N stretching mode was found to be underestimated, while ν(Pd-Cl) and ν(NH_3/NH_2) were overestimated. Hence, this lack

of accordance is independent of the type of complex investigated, the main issue probably remaining to be the description of the modes involving the metal center.

Additionally, neither the AE approach to describe the metal center nor the two-molecule model calculations led to a noticeable improvement of the corresponding vibrational modes. In fact, it was previously verified by the authors[17] that an enhancement in the calculated structural parameters is not always accompanied by a corresponding improvement of the accuracy of the vibrational frequencies.

4. CONCLUSIONS

In the present work, a complete vibrational study of a dinuclear Pd(II) complex displaying a promising antiproliferative activity was undertaken, by a combined spectroscopic and quantum mechanical calculations methodology. FTIR, Raman and INS spectra were recorded and the theoretical analysis was carried out at the DFT level, for both the isolated molecule and a two-molecule model.

It was shown that the intermolecular interactions within the crystal lattice are of the utmost importance for this type of polynuclear polyamine chelates. A simple isolated molecule calculation was found not to suffice for predicting the molecular properties of such a system, as opposed to what has been reported (by the authors) for their mononuclear counterparts. Although the calculations performed for the two-molecule species yielded slightly better results, the structural improvements were not noteworthy. Furthermore, whenever there are no X-ray data available and several possible two-molecule geometries to be tested, this type of approach becomes excessively demanding (in terms of computational costs).

In order to further improve the representation of this kind of Pd(II)-amine complexes, it is of paramount importance to develop new basis sets as was recently carried out for Pt(II) complexes[19,41] (which was out of the scope of this work). At the moment, it seems that the precise estimate of one type of metal-ligand bond length leads to the unbalance of the other one, and an improvement of the bond lengths implies a worse description of the bond angles. Therefore, when considering only the prediction of the structural parameters, some doubts can arise as to the most suitable theoretical approach. For the representation of the vibrational profiles, in turn, the LANL2DZ/6-31G* functional was shown to attain a high degree of accordance with the experiment, while the enhancement obtained with higher theory levels was not worth the associated computational cost. Optimization of the theoretical methodology for this kind of polynuclear polyamine Pd(II) agents will hopefully allow the establishment of accurate and reliable SAR's and to predict other important properties relevant for their anticancer capacity. Finally, while plane-wave calculations are of utmost importance for estimating the properties of a molecule in the solid state, an up-to-date all-electron basis set for palladium(II) is also crucial, since studies for an isolated molecule cannot be ruled out for large polynuclear complexes bearing biological properties.

The data obtained in this work shows an inverse relationship between the strength of the Pd-Cl bond and the antiproliferative effect of Pd_2-Spm against cancer cells, i.e., the weaker the Pd-Cl bonds the higher the complex's activity. The antiproliferative activity of such a compound is determined by several other factors. However, this evidence may indicate that these Pd(II)-amine chelates (comprising cisplatin-like moieties) could display a similar mode of action to that of cisplatin, involving chloride hydrolysis inside the cell as their major activation step.

Acknowledgements

The authors acknowledge financial support from the Portuguese Foundation for Science and Technology – PEst-OE/QUI/UI0070/2014. SF thanks FCT - the Portuguese Foundation for Science and Technology – SFRH/BPD/75334/2010 scholarship. The STFC Rutherford Appleton Laboratory is thanked for access to neutron beam facilities. The INS work was supported by the European Commission under the 7th Framework Programme through the Key Action: Strengthening the European Research Area, Research Infrastructures (Contract n°: CP-CSA_INFRA-2008-1.1.1 Number 226507-NMI3). Laboratório Associado CICECO (University of Aveiro, Portugal) is also acknowledged for access to the FT-Raman and FTIR spectrometers.

References

1 S. Ray, R. Mohan, J. K. Singh, M. K. Samantaray, M. M. Shaikh, D. Panda, and P. Ghosh, *J. Am. Chem. Soc.* 2007, **129**, 15042-15053.
2 E. Gao, C. Liu, M. Zhu, H. Lin, Q. Wu and L Liu,. *Anti-cancer Agents Med. Chem.* 2009, **9**, 356-368.
3 F. Aria, B. Cevatemrea, E. I. I. Armutakb, N. Aztopala, V.T. Yilmazc and E. Ulukaya, *Bioorg. Med. Chem*. 2014, 22, 4948–4954.
4 A. Garoufis, S. K. Hadjikakou and N. Hadjiliadis, *Coord. Chem. Rev.* 2009, **253**, 1384-1397.
5 E. Sindhuja, R. Ramesh, N. Dharmaraj and Y. Liu, *Inorg Chim Acta* 2014, **416**, 1-12.
6 J. L. Butour, S. Wimmer, F. Wimmer and P. Castan, *Chem.-Biol. Interact.* 1997, **104**, 165-178.
7 F. Shaheen, A. Badshah, M. Gielen, C. Gieck, M. Jamil and D. Vos, *J. Organomet. Chem.* 2008, **693**, 1117-1126.
8 F. Shaheen, A. Badshah, M. Gielen, G. Croce, U. Florke, D. de Vos and S. Ali, *J. Organomet. Chem.* 2010, **695**, 315-322.
9 H. A. El-Asmy, I. S. Butler, Z. S. Mouhri, B. J. Jean-Claude, M. S. Emmam and S. I. Mostafa, *J. Mol. Struct.* 2014, **1059**, 193–201.
10 P. Vranec and I. Potocnak, *J. Mol. Struct.* 2013, **1041**, 219-226.
11 R. A. Haque, A. W. Salman, S. Budagumpi, A. A. A. Abdullah and A. M. S. A. Majid, *Metallomics* 2013, **5**, 760-769.
12 M. P. M. Marques, *ISRN Spectrosc.* 2013, **2013**, 1-29.
13 D. Kovala-Demertzi, A. Alexandratos, A. Papageorgiou, P. N. Yadav, P. Dalezis and M. A. Demertzis, *Polyhedron* 2008, **27**, 2731-2738.
14 G. Codina, A. Caubet, C. López, V. Moreno and E. Molins, *Helv. Chim. Acta* 1999, **82**, 1025.
15 A. S. Soares, S. M. Fiuza, M. J. Gonçalves, L. A. E. Batista de Carvalho, M. P. M. Marques and A. M. Urbano, *Lett. Drug Des. Disc.* 2007, **4**, 460-463.
16 S. M. Fiuza, J. Holy, L. A. E. Batista de Carvalho and M. P. M. Marques, *Chem. Biol. Drug Des.* 2011, **77**, 477–488.
17 S. M. Fiuza, A. M. Amado, H. F. Dos Santos, M. P. M. Marques and L. A. E. Batista de Carvalho, *Phys. Chem. Chem. Phys.* 2010, **12**, 14309-14321.

18 A. M. Amado, S. M. Fiuza, M. P. M. Marques and L. A. E. Batista de Carvalho, *J. Chem. Phys.* 2007, **127**, 185104.
19 D. Paschoal, B. L. Marcial, J. F. Lopes, W. B. De Almeida and H. F. Dos Santos, *J. Comp. Chem.* 2012, **33**, 2292-2302.
20 http://www.isis.stfc.ac.uk/
21 M. J. Frisch, G. W. Trucks, H. B. Schlegel, G. E. Scuseria, M. A. Robb, J. R. Cheeseman, J. A. Montgomery Jr., T. Vreven, K. N. Kudin, J. C. Burant, J. M. Millam, S. S. Iyengar, J. Tomasi, V. Barone, B. Mennucci, M. Cossi, G. Scalmani, N. Rega, G. A. Petersson, H. Nakatsuji, M. Hada, M. Ehara, K. Toyota, R. Fukuda, J. Hasegawa, M. Ishida, T. Nakajima, Y. Honda, O. Kitao, H. Nakai, M. Klene, X. Li, J. E. Knox, H. P. Hratchian, J. B. Cross, V. Bakken, C. Adamo, J. Jaramillo, R. Gomperts, R. E. Stratmann, O. Yazyev, A. J. Austin, R. Cammi, C. Pomelli, J. W. Ochterski, P. Y. Ayala, K. Morokuma, G. A. Voth, P. Salvador, J. J. Dannenberg, V. G. Zakrzewski, S. Dapprich, A. D. Daniels, M. C. Strain, O. Farkas, D. K. Malick, A. D. Rabuck, K. Raghavachari, J. B. Foresman, J. V. Ortiz, Q. Cui, A. G. Baboul, S. Clifford, J. Cioslowski, B. B. Stefanov, G. Liu, A. Liashenko, P. Piskorz, I. Komaromi, R. L. Martin, D. J. Fox, T. Keith, M. A. Al-Laham, C. Y. Peng, A. Nanayakkara M. Challacombe, P. M. W. Gill, B. Johnson, W. Chen, M. W. Wong, C. Gonzalez and J. A. Pople, Gaussian 03, Revision D.01, Gaussian, Inc., Wallingford, CT, 2004.
22 P. J. Hay and W. R. Wadt, *J. Chem. Phys.* 1985, **82**, 299-310.
23 M. E. Friedlander, J. M. Howell and G. Snyder, *J. Chem. Phys.* 1982, **77**, 1921-1929.
24 A. W. Ehlers, M. Bohme, S. Dapprich, A. Gobbi, A. Hollwarth, V. Jonas, K. F. Kohler, R. Stegmann, A. Veldkamp and G. Frenking, *Chem. Phys. Lett.* 1993, **208**, 111-114.
25 C. Adamo and V. Barone *J. Chem. Phys.* 1998, **108**, 664-675.
26 J. P. Perdew, K. Burke and Y. Wang, *Phys. Rev. B* 1996, **54**, 16533.
27 S. Padrão, S. M. Fiuza, A. M. Amado, A. M. A. da Costa and L. A. E. Batista de Carvalho, *J. Phys. Org. Chem.* 2011, **24**, 110-121.
28 S. Grimme, *J. Comp. Chem.* 2006, **27**, 1787-1799.
29 S. F. Boys and F. Bernardi, *Mol. Phys.*1970, **19**, 558-566.
30 R. L. Lopes, M. P. M. Marques, R. Valero, J. Tomkinson and L. A. E. Batista de Carvalho, *Spectrosc. Int. J.* 2012, **27**, 273-292.
31 M. P. M. Marques, R. Valero, S. F. Parker, J. Tomkinson and L. A. E. Batista de Carvalho, *J. Phys. Chem. B* 2013, **117**, 6421- 6429.
32 R. L. Lopes, R. Valero, J. Tomkinson, M. P. M. Marques and L. A. E. Batista de Carvalho, *New J. Chem* 2013, **37**, 2691–2699.
33 M. P. M. Marques, L. A. E. Batista de Carvalho, R. Valero, N. F. L. Machado and S. F. Parker, *Phys. Chem. Chem. Phys.* 2014, **16**, 7491-7500.
34 S. D. Kirik, L. A. Solovyov and M. L. Blokhina, *Acta Cryst.* 1996, **B52**, 909-916.
35 P. Banerjee, *Coord. Chem. Rev.* 1999, **190-192**, 19-28.
36 A. Eastman, *Biochem.* 1983, **22**, 3927-3933.
37 M. Kartalou and J. M. Essigmann, *Mut. Res.* 2001, **478**, 1-21.
38 J. P. Merrick, D. Moran and L. Radom, *J. Phys. Chem. A*, 2007, **111**, 11683–11700.
39 M. P. M. Marques, L. A. E. Batista de Carvalho and J. Tomkinson, *J Phys. Chem. A* 2002, **106**, 2473-2482.

40 L. A. E. Batista de Carvalho, M. P. M. Marques and J. Tomkinson, *J Phys. Chem. A* 2006, **110**, 12947-12954.
41 R. C. De Berrêdo and F. E. Jorge, *J. Mol. Struct. Theochem* 2010, **961**, 107-112.

TABLE 1 - Theoretical levels considered in this study.

System	Basis Set		
	Pd(II)[a]	Non-heavy atoms[b]	
Two-molecule model	LANL2DZ	6-31G*	
Isolated molecule	AE	6-31G*	
	AE	6-31G**	
	AE	6-31+G(2df)	
	AE	6-31G** (H) 6-31G* (C) 6-31+G(2d) (N) 6-31+G(2df) (Cl)	mix1
	AE	6-31G** (H) 6-31+G(2d) (C,N) 6-31+G(2df) (Cl)	mix2

[a] AE stands for the all electron basis set of Friedlander[23] used at the Pd(II) ion.
[b] Basis sets used generally or specifically on each atom as specified in mix1 and mix2.

TABLE 2: Experimental and calculated structural parameters for Pd_2-Spm, at different theoretical levels.

		Theory Level[c]											
Structural Parameter	**Exp**[a]	**LANL2DZ/ 6-31G***	**Δ**[b]	**AE/ 6-31G***	**Δ**[b]	**AE/ 6-31G****	**Δ**[b]	**AE/ 6-31G+(2d)**	**Δ**[b]	**AE/mix1**	**Δ**[b]	**AE/mix2**	**Δ**[b]
Bond Length/pm													
$Pd\text{-}N_1$	**202.2**	208.4	**6.2**	205.3	**3.1**	205.3	**3.1**	205	**2.8**	204.7	**2.5**	206.1	**3.9**
$Pd\text{-}N_2$	**204.1**	209.8	**5.7**	205.7	**1.6**	205.2	**1.1**	205.5	**1.4**	205.1	**1.0**	205.5	**1.4**
$Pd\text{-}Cl_1$	**231.6**	231.7	**0.1**	232.8	**1.2**	227.9	**-3.7**	233	**1.4**	232.4	**0.8**	228.7	**-2.9**
$Pd\text{-}Cl_2$	**231.4**	232.2	**0.8**	233.8	**2.4**	229.2	**-2.2**	233.9	**2.5**	233.3	**1.9**	230.6	**-0.8**
$N_1\text{-}C_1$	**148.5**	147.8	**-0.7**	147.2	**-1.3**	147.1	**-1.4**	147.2	**-1.3**	147.3	**-1.2**	147	**-1.5**
$N_2\text{-}C_3$	**148.7**	147.5	**-1.2**	147.1	**-1.6**	147.3	**-1.4**	147	**-1.7**	147.1	**-1.6**	146.9	**-1.8**
$C_1\text{-}C_2$	**150.6**	152.4	**1.8**	152.5	**1.9**	152.4	**1.8**	152.5	**1.9**	152.5	**1.9**	152.3	**1.7**
$C_2\text{-}C_3$	**151.8**	152.7	**0.9**	152.8	**1.0**	152.6	**0.8**	152.8	**1.0**	152.8	**1.0**	152.6	**0.8**
$C_4\text{-}C_5$	**152.1**	152.1	**0.0**	152.3	**0.2**	152.1	**0.0**	152.3	**0.2**	152.3	**0.2**	152	**-0.1**
$C_5\text{-}C_6$	**153.3**	152.6	**-0.7**	151.5	**-1.8**	152.4	**-0.9**	151.5	**-1.8**	151.5	**-1.8**	152	**-1.3**
$N_2\text{-}C_4$	**148.8**	147.8	**1.0**	147.8	**-1.0**	147.4	**-1.4**	147.7	**-1.1**	147.8	**-1.0**	147	**-1.8**
Angles/º													
$Cl_1\text{-}Pd\text{-}Cl_2$	**93.9**	96.3	**2.4**	99.2	**5.3**	97	**3.1**	99.5	**5.6**	99.1	**5.2**	97.7	**3.8**
$N_1\text{-}Pd\text{-}N_2$	**90.3**	92	**1.7**	91.9	**1.6**	91.8	**1.5**	92.1	**1.8**	92	**1.7**	91.7	**1.4**
$N_1\text{-}Pd\text{-}Cl_1$	**88.5**	85.5	**-3.0**	84.3	**-4.2**	85.5	**-3.0**	84	**-4.5**	84.3	**-4.2**	85.6	**-2.9**
$N_2\text{-}Pd\text{-}Cl_2$	**87.5**	86.1	**-1.4**	84.5	**-3.0**	85.7	**-1.8**	84.2	**-3.3**	84.5	**-3.0**	85	**-2.5**
$Pd\text{-}N_1\text{-}C_1$	**114.8**	113.8	**-1.0**	108.5	**-6.3**	113.2	**-1.6**	108.5	**-6.3**	108.5	**-6.3**	113.1	**-1.7**
$Pd\text{-}N_2\text{-}C_3$	**113.9**	111.8	**-2.1**	112.4	**-1.5**	111.9	**-2.0**	112.4	**-1.5**	112.4	**-1.5**	112.5	**-1.4**
$Pd\text{-}N_2\text{-}C_4$	**113**	115.5	**2.5**	112.1	**-0.9**	115.3	**2.3**	112.1	**-0.9**	112.1	**-0.9**	114.1	**1.1**
$N_1\text{-}C_1\text{-}C_2$	**110.5**	112.5	**2.0**	112.3	**1.8**	112.2	**1.7**	112.3	**1.8**	112.2	**1.7**	112.7	**2.2**
$N_2\text{-}C_3\text{-}C_2$	**114.3**	114.5	**0.2**	114.4	**0.1**	114.1	**-0.2**	114.3	**0.0**	114.3	**0.0**	114.2	**-0.1**
$C_1\text{-}C_2\text{-}C_3$	**115.7**	115.9	**0.2**	116.4	**0.7**	115.8	**0.1**	116.4	**0.7**	116.4	**0.7**	116	**0.3**
$C_3\text{-}N_2\text{-}C_4$	**113**	113.7	**0.7**	115.1	**2.1**	113.9	**0.9**	115.2	**2.2**	115	**2.0**	114.2	**1.2**
$N_2\text{-}C_4\text{-}C_5$	**112.3**	112.3	**0.0**	109.6	**-2.7**	111.7	**-0.6**	109.6	**-2.7**	109.6	**-2.7**	112	**-0.3**
$C_4\text{-}C_5\text{-}C_6$	**111.3**	111.2	**0.1**	113	**1.7**	111.5	**0.2**	113.1	**1.8**	113	**1.7**	111.3	**0.0**
ΔΔ			**1.5**		**2.0**		**1.5**		**2.1**		**1.9**		**1.5**

[a] Average values for identical bonds in the molecule[14]. [b] Δ = Calculated value–Experimental value[18]

TABLE 3: Experimental (INS, Raman, FTIR) and calculated (LANL2DZ/6-31G*) vibrational wavenumbers (cm^{-1}) for Pd_2-Spm (isolated molecule).

Experimental			Calculated	Scaled[a]	Sym.	Tentative assignment[c]
INS	Raman	FTIR				
		3253	3588	3408/3337[b]	A_u	$\nu_{as}NH_2$
	3221		3588	3408/3337[b]	A_g	$\nu_{as}NH_2$
		3215	3484	3309/3240[b]	A_u	νNH
			3484	3309/3240[b]	A_g	νNH
		3142	3483	3309/3239[b]	A_u	$\nu_{s}NH_2$
	3146		3483	3309/3239[b]	A_g	$\nu_{s}NH_2$
			3165	3006	A_u	$\nu_{as}CH_{2\ (ring)}$
			3165	3006	A_g	$\nu_{as}CH_{2\ (ring)}$
			3150	2992	A_u	$\nu_{as}CH_{2\ (chain)}$
		2960	3137	2980	A_u	$\nu_{as}CH_{2\ (ring)}$
	2960		3137	2980	A_g	$\nu_{as}CH_{2\ (ring)}$
2950	2948		3130	2973	A_g	$\nu_{as}CH_{2\ (chain)}$
	2935		3126	2969	A_g	$\nu_{as}CH_{2\ (ring)}$
		2935	3126	2969	A_u	$\nu_{as}CH_{2\ (ring)}$
			3112	2956	A_u	$\nu_{as}CH_{2\ (chain)}$
	2922		3110	2954	A_g	$\nu_{as}CH_{2\ (chain)}$
			3092	2937	A_u	$\nu_{s}CH_{2\ (chain)}$
			3087	2932	A_g	$\nu_{s}CH_{2\ (ring)}$
			3087	2932	A_u	$\nu_{s}CH_{2\ (ring)}$
			3085	2930	A_g	$\nu_{s}CH_{2\ (ring)}$
			3085	2930	A_u	$\nu_{s}CH_{2\ (ring)}$
	2878		3083	2929	A_g	$\nu_{s}CH_{2\ (chain)}$
			3078	2924	A_u	$\nu_{s}CH_{2\ (ring)}$
			3078	2924	A_u	$\nu_{s}CH_{2\ (ring)}$
	2864		3051	2898	A_g	$\nu_{s}CH_{2\ (chain)}$
		2865	3051	2898	A_u	$\nu_{s}CH_{2\ (chain)}$
	1595		1699	1614/1580[b]	A_g	δNH_2
1601		1596	1699	1614/1580[b]	A_u	δNH_2
			1539	1462	A_u	$\delta CH_{2\ (chain)}$
	1469		1537	1460	A_g	$\delta CH_{2\ (chain)}$
		1458	1529	1452	A_u	$\delta CH_{2\ (ring)}$
1457	1454		1527	1450	A_g	$\delta CH_{2\ (ring)}$
		1449	1524	1448	A_u	$\delta CH_{2\ (ring)}$
	1442		1523	1447	A_g	$\delta CH_{2\ (ring)}$
1440			1511	1435	A_u	$\delta CH_{2\ (ring)}$
			1508	1432	A_g	$\delta CH_{2\ (ring)}$
		1434	1508	1432	A_u	$\delta CH_{2\ (ring)}$
	1430		1504	1429	A_g	$\delta CH_{2\ (chain)}$
			1486	1412	A_g	βNH
			1485	1411	A_u	βNH
	1386		1460	1387	A_g	$\omega CH_{2\ (chain)}$
1385		1377	1455	1382	A_u	$\omega CH_{2\ (chain)}$
	1372		1436	1364	A_g	$\omega CH_{2\ (ring)}$
1365			1432	1360	A_u	$\omega CH_{2\ (ring)}$
	1367		1431	1359	A_g	$\omega CH_{2\ (ring)}$
		1355	1424	1353	A_u	$\omega CH_{2\ (ring)}$
1351	1351		1406	1336	A_g	$\omega CH_{2\ (ring)}$
1338			1398	1328	A_u	$\omega CH_{2\ (ring)}$
		1317	1377	1308	A_u	$tCH_{2\ (chain)}$
1314	1317		1372	1303	A_g	$tCH_{2\ (ring)}$
1299	1304		1371	1302	A_g	$\omega CH_{2\ (chain)}$

		1293	1368	1299	A_u	$tCH_{2\ (ring)}$
			1361	1293	A_g	$tCH_{2\ (chain)}$
1278	1273		1348	1280	A_g	$tCH_{2\ (chain)}$
1256		1264	1334	1267	A_u	$tCH_{2\ (ring)}$
1240		1238	1304	1239	A_u	$\omega CH_{2\ (chain)}$
1218	1224		1295	1230	A_g	$tCH_{2\ (ring)}$
	1213		1287	1223	A_g	$tCH_{2\ (ring)}$
		1213	1281	1217	A_u	$tCH_{2\ (ring)}$
1163		1179	1261	1198	A_u	$tNH_2 + tCH_{2\ (chain)}$
	1185		1244	1182	A_g	$tNH_2 + \rho CH_{2\ (chain)}$
		1146	1184	1125	A_u	$tCH_{2\ (chain)} + tCH_{2\ (ring)}$
	1147		1167	1109	A_g	νC-C
1136	1131		1166	1108	A_g	$\rho CH_{2\ (chain)}$
		1133	1163	1105	A_u	ωNH_2
	1120		1142	1085	A_g	νC-C
			1130	1073	A_u	νC-N
	1108		1127	1071	A_g	ωNH_2
1085		1085	1122	1066	A_u	νC-N
			1107	1052	A_u	νC-N
1070	1064		1100	1045	A_g	$\nu C\text{-}C_{(chain)}$
1057	1055		1098	1043	A_g	νC-N
		1057	1092	1037	A_u	νC-N
			1082	1028	A_g	γNH
			1065	1012	A_u	γNH
			1058	1005	A_g	νC-C
			1052	999	A_g	νC-N
		969	1025	974	A_u	νC-C
		918	977	928	A_u	νC-C
930	932		970	921	A_g	$\rho CH_{2(ring)}$
		899	945	898	A_u	$\rho CH_{2(chain)}$
906			939	892	A_u	$\rho CH_{2\ (ring)}$
	903		937	890	A_g	$\rho CH_{2(ring)}$
	861		884	840	A_g	$\rho CH_{2\ (ring)}$
		862	883	839	A_u	$\rho CH_{2\ (ring)}$
812	814		826	785	A_g	$\rho CH_{2\ (ring)}$
789		790	823	782	A_u	$\rho CH_{2\ (ring)}$
			811	770	A_g	$\rho CH_{2\ (chain)}$
			750	712	A_u	$\rho CH_{2\ (chain)}$
707/725/745		706/739	680	680	A_u	ρNH_2
	703/740		680	680	A_g	ρNH_2
612	598		572	572	A_g	β ring
576		579	560	560	A_u	β ring
544		552	549	549	A_u	δ N-C-$C_{(ring)}$
	514		531	531	A_g	δ C-N-C
			474	474	A_u	δ C-N-C
504	501	502	437	485[b]	A_u	ν_sPd-N
			436	484[b]	A_g	ν_sPd-N
457	464		471	471	A_g	$\tau\ CC_{ring}$
450	449		398	442[b]	A_g	ν_{as}Pd-N
442		449	393	436[b]	A_u	ν_{as}Pd-N
	324	-	345	321[b]	A_g	ν_s Pd-Cl
		-	343	319[b]	A_u	ν_s Pd-Cl
361/375		-	337	337	A_u	γ ring
	309	-	326	303[b]	A_g	ν_{as} Pd-Cl
295		-	315	293[b]	A_u	ν_{as} Pd-Cl
286	276	-	282	262[b]	A_g	δ N-Pd-N

		-	281	261[b]	A_u	δ N-Pd-N
242	256	-	265	265	A_g	γ ring
236	237	-	249	249	A_g	β C-C-C "swinging"
216		-	222	222	A_u	"ring breathing"
		-	198	198	A_u	γ_1 C-C-C_{chain}
196	203	-	185	205[b]	A_g	δ N-Pd-Cl
		-	179	199[b]	A_u	δ N-Pd-Cl
168	164	-	167	167	A_g	τ C-N_{ring}
153	152	-	150	150	A_g	γ_2 C-C-C_{chain}
160		-	148	148	A_u	γ_3 C-C-C_{chain}
		-	142	142	A_u	δ Cl-Pd-Cl
		-	140	140	A_g	δ Cl-Pd-Cl
		-	127	127	A_g	γ_4 C-C-C_{chain}
117		-	121	121	A_u	τ C-N_{ring}
103		-	104	104	A_g	γ_5 C-C-C_{chain}
		-	89	89	A_u	γ N-Pd-Cl
		-	88	88	A_g	γ N-Pd-Cl
		-	75	75	A_u	γ' N-Pd-Cl
		-	74	74	A_g	γ' N-Pd-Cl
		-	70	70	A_u	Skeletal modes
		-	52	52	A_g	Skeletal modes
30		-	32	32	A_u	Skeletal modes
25		-	26	26	A_g	Skeletal modes
		-	23	23	A_u	Skeletal modes
		-	11	11	A_u	Skeletal modes

[a]Wavenumbers above 700 cm^{-1} were scaled accordingly to Merrick *et al.*[38] using a scaling factor of 0.9499. [b]Wavenumbers scaled according to Fiuza *et al.*[17] [c]ν = stretching; δ, β = in-plane deformation; ρ = rocking; τ = torsion; γ and γ'=in phase and out of phase out-of-plane deformation.

TABLE 4: Calculated (LANL2DZ/6-31G*) scaling factors for selected vibrational modes of several Pd(II)-amine complexes.

	Scaling factor for each vibrational mode		
Compound	**$\nu NH_3/\nu NH_2$**	**νPd-N**	**νPd-Cl**
cDDPd	0.91	1.13	0.93
$[Pd(NH_3)_4]\cdot 2Cl\cdot H_2O$	0.93	1.10	–
$[Pd(NH_3)_3(DMSO)]\cdot 2Cl$	0.92	1.11	–
$[PdCl_2(en)]$	0.91	1.07	0.90
$[PdCl_2(dap)]$	0.92	1.20	0.89
$[Pd_2\text{-Spm}]$	0.92	1.17	0.94
Average	0.92	1.13	0.92

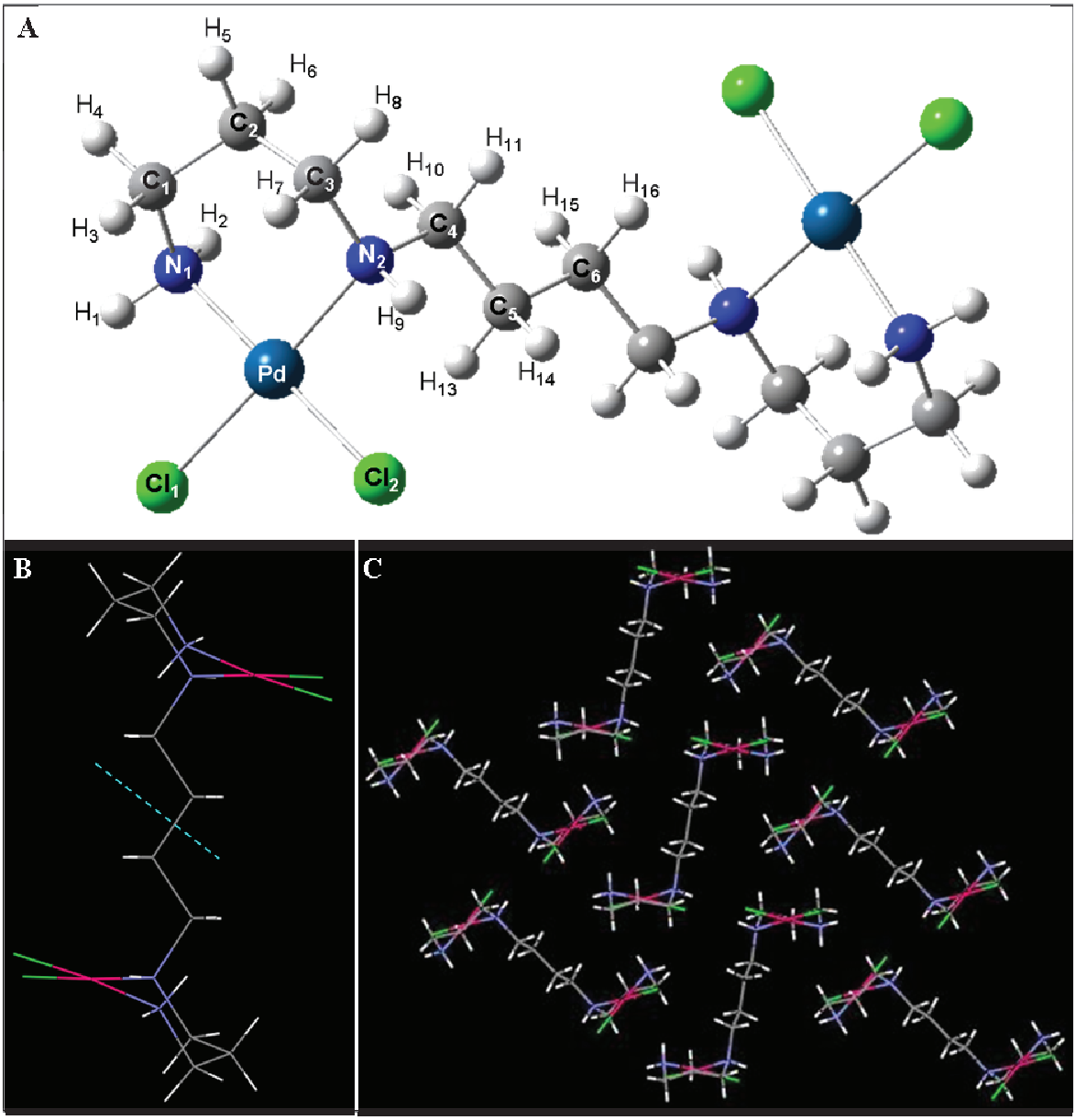
A
H5
H6
H8
H4
C2
H11
H10
C1
H7
C3
H15
H16
H2
C4
H3
N1
N2
C6
H1
H9
C5
Pd
H13
H14
Cl1
Cl2
B
C

Figure 1 – **A** Optimized structure (LANL2DZ/6-31G*) for the Pd_2-Spm isolated molecule, and corresponding atom numbering. **B** X-ray structure for Pd_2-Spm. (Preferred conformation in the solid state with the inversion center highlighted by the blue dashed line). **C** Crystal structure arrangement for Pd_2-Spm.

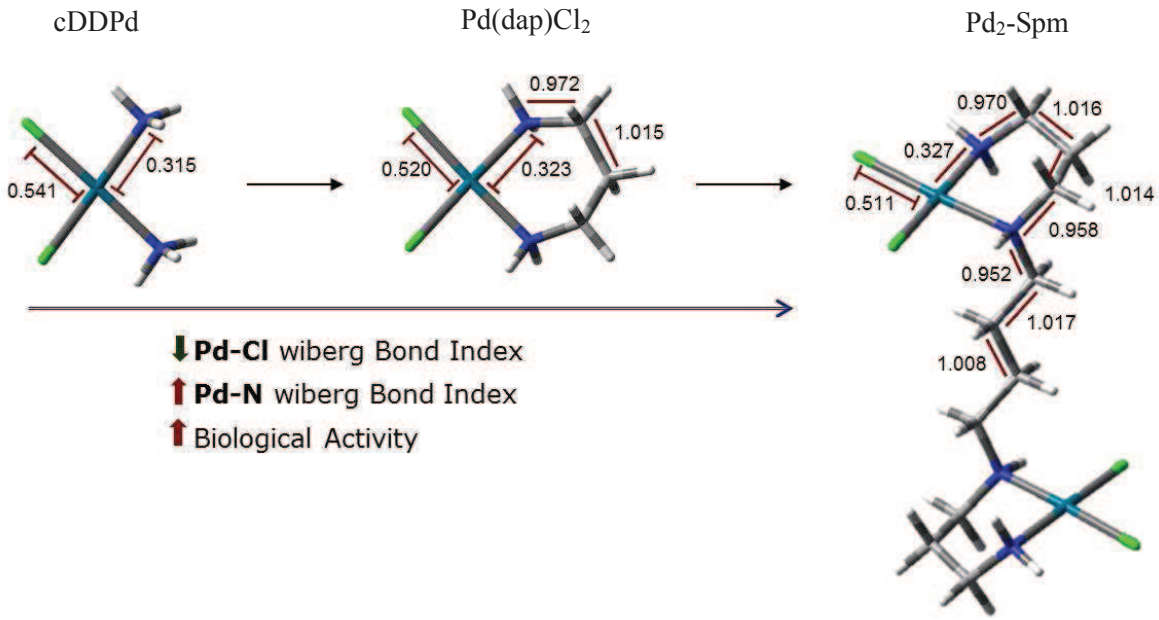

Figure 2 - Variation of Wiberg bond indexes (WBI) for three different Pd(II) complexes: cDDPd (cis-diamminodichloropalladium(II) $Pd(dap)Cl_2$ (1,3-diamminopropanepalladium(II) chloride) and Pd_2-Spm. (Green – Cl; Cyan – Pd(II); Blue – N).

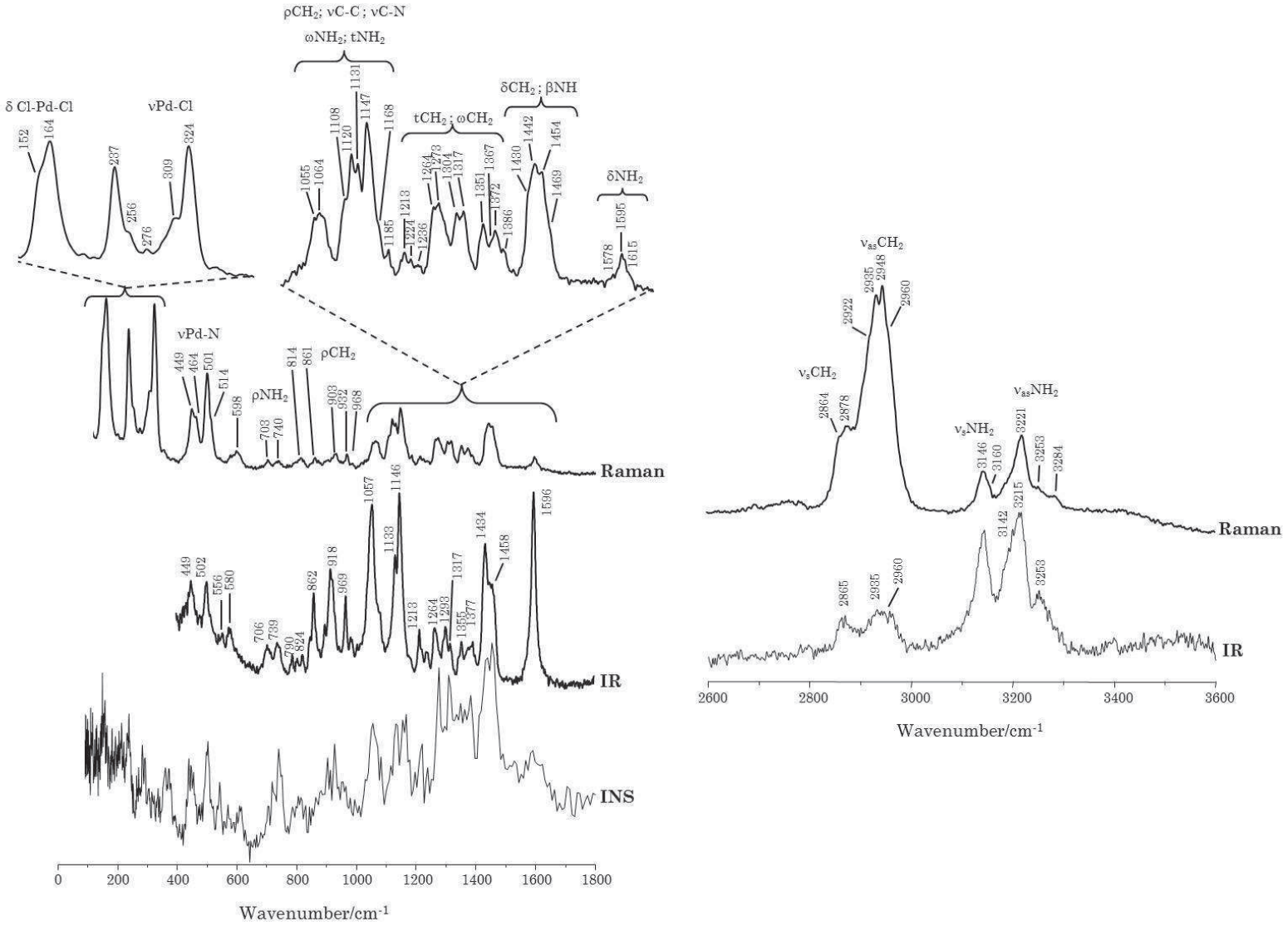

Figure 3 – Experimental vibrational spectra (Raman, IR and INS) for Pd_2-Spm.

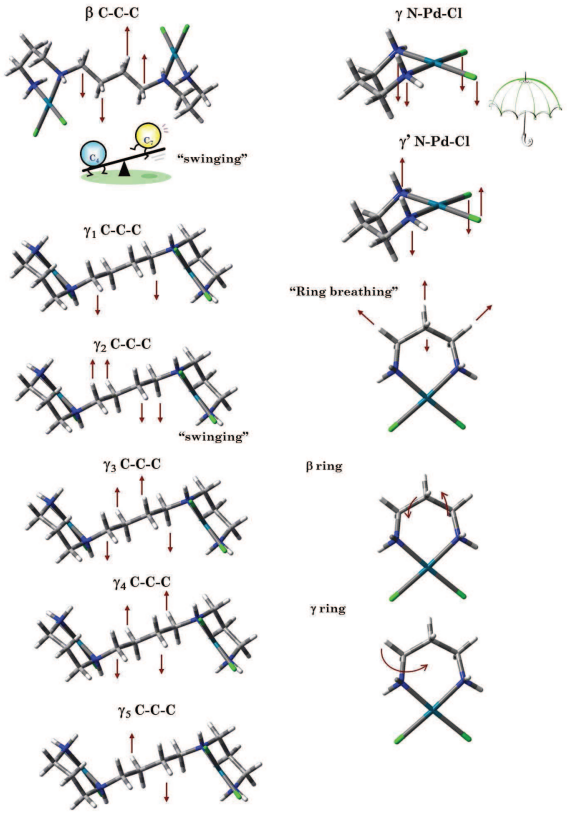

Figure 4 – Schematic representation of selected vibrational modes for Pd_2-Spm (and nomenclature used along this work).

Figure S1 – Conformational study of Pd_2-Spm. Input geometries are listed with letters and the obtained conformers are listed in arabic numbers from 1 to 19 on increasing energy and thus from the most stable to the less stable one. A graphic with the relative energies is presented.

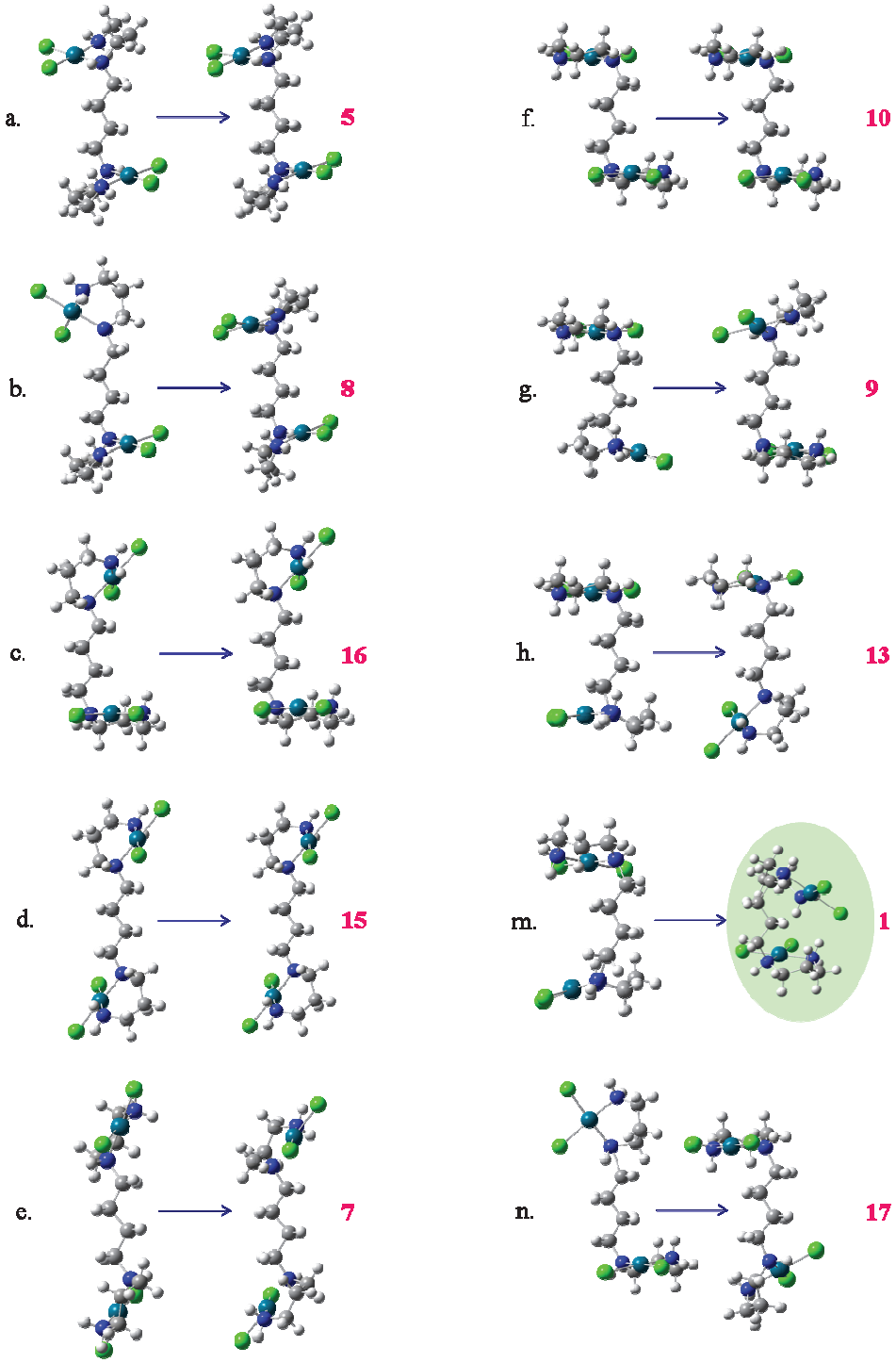

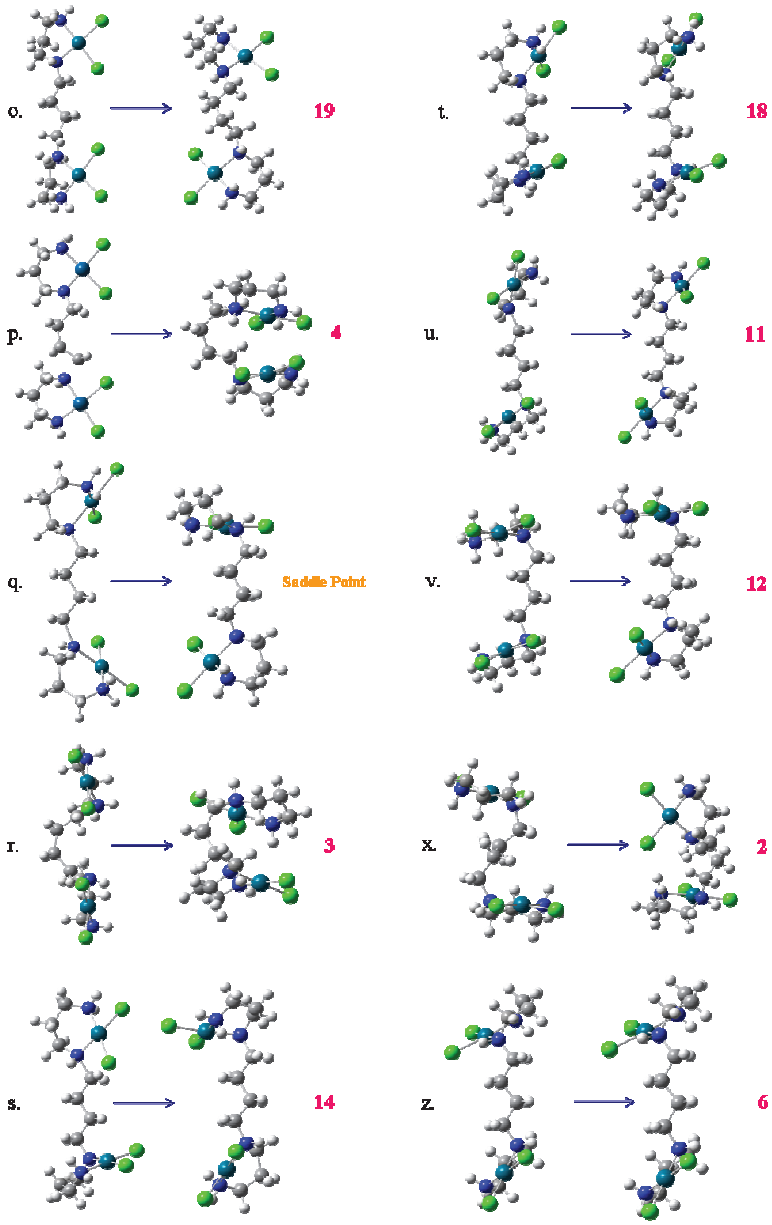
o.
19
t.
18
p.
4
u.
11
q.
Saddle Point
v.
12
r.
3
x.
2
s.
14
z.
6

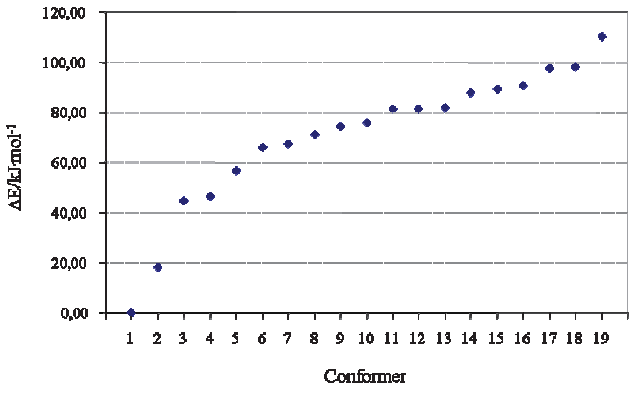
120,00
100,00
80,00
60,00
40,00
20,00
0,00
ΔE/kJmol-1
1 2 3 4 5 6 7 8 9 10 11 12 13 14 15 16 17 18 19
Conformer

Figure S2 – Calculated two molecule structure for Pd_2-Spm.
(The distance between atoms is in picometers).